

A nitrogen-enriched nebula around P Cygni

Dean R. H. Johnson,¹* M. J. Barlow,² J. E. Drew¹ and Elias Brinks³

¹Department of Astrophysics, University of Oxford, Nuclear Physics Building, Keble Road, Oxford OX1 3RH

²Department of Physics and Astronomy, University College London, Gower Street, London WC1E 6BT

³National Radio Astronomy Observatory, PO Box 0, Socorro, New Mexico 87801, USA

Accepted 1991 October 14. Received 1991 October 8; in original form 1991 August 12

SUMMARY

We have detected extended nebular emission in [S II] $\lambda\lambda$ 6716, 6731, [N II] λ 6584, 6548 and H α on a long-slit spectrum offset by 9 arcsec from P Cyg. Anomalously strong [Ni II] λ 6666.8 emission was also detected. The [S II] doublet ratio yields an electron density of 600 cm^{-3} . The [N II] and [S II] lines have been used to derive an N/S ratio which is insensitive to the adopted value of electron temperature. The N/S ratio is 33 ± 5 by number, five times higher than solar, implying that the material has undergone CN-cycle processing which has converted most of the original carbon into nitrogen.

1 INTRODUCTION

P Cygni, along with η Carinae and S Doradus, is one of the prototypes of a group of stars now classed together as luminous blue variables (LBVs; see Davidson, Moffat & Lamers 1989). Amongst the properties of these stars (Humphreys 1989) are: (i) optical spectra (which may vary between late O- and A-type) which exhibit well-developed P Cygni profiles, implying large mass-loss rates; (ii) very high luminosities, and (iii) photometric variability with a variety of amplitudes and time-scales. Many LBVs also show evidence of circumstellar nebular ejecta, with abundance analyses of these ejecta pointing to large nitrogen enhancements, indicative of CNO-cycle processed material exposed by mass loss from these massive stars. Examples include the η Carinae homunculus (Davidson *et al.* 1986), the AG Carinae ring nebula (Mitra & Dufour 1990) and a number of LBVs in the Large Magellanic Cloud (LMC) (Walborn 1982; Stahl & Wolf 1986).

Wendker (1982) and Baars & Wendker (1987) have detected an arc of faint, apparently thermal, radio emission about 30 arcsec to the north-west of P Cyg, which has not yet been observed at optical wavelengths.

Leitherer & Zickgraf (1987) imaged P Cygni in narrow-band H α , [N II] 6584 Å and continuum interference filters using a CCD with $0.46 \text{ arcsec pixel}^{-1}$. By comparing azimuthally averaged radial surface-brightness profiles with those obtained for the similar apparent brightness star 55 Cyg, they found evidence for excess radial emission in both H α and [N II], with a θ^{-3} surface-brightness distribution out to about 7 arcsec, where θ is the angular separation from the

star. This brightness distribution could be fitted by emission from an r^{-2} density distribution, where r is the distance from the star. The required steady mass-loss rate was, however, about a factor of 10 higher than that derived from radio measurements of P Cygni, leading Leitherer & Zickgraf to invoke filling-factor effects associated with the hypothesized periodic ejection of shells by P Cygni.

Stahl (1989) reported long-slit CCD spectroscopy of P Cygni obtained by Zickgraf and himself using a slit width of 0.5 arcsec and a pixel size perpendicular to the dispersion of 0.2 arcsec. They determined the angular distribution of emission for a wavelength bin centred on [N II] 6584 Å, after subtracting the average flux from two continuum bins of equal wavelength extent on either side of the [N II] line. Beyond an angular radius of 1.5 arcsec they found no evidence for excess [N II] emission. The upper limit quoted by Stahl for the [N II] surface brightness at an angular radius of 2 arcsec was a factor of 5 lower than that determined by Leitherer & Zickgraf (1987). Stahl suggested that undersampling of the peak of the seeing profile by Leitherer & Zickgraf might have been the cause of the discrepancy, though noting that the azimuthally averaged measurements of the latter might have picked up asymmetrically distributed emission that was not encountered by his own long slit, whose position angle was unfortunately not quoted.

We report here long-slit spectra obtained at a number of offset positions close to P Cygni, which unambiguously detect nebular [N II] and [S II] emission.

2 OBSERVATIONS

Long-slit red spectra were obtained on 1988 October 11 UT using the 500-mm camera of the Intermediate Dispersion

*Present address: Department of Physics and Astronomy, University of Wales College of Cardiff, PO Box 913, Cardiff CF1 3TH.

Spectrograph mounted at the Cassegrain focus of the 2.5-m Isaac Newton Telescope at the Observatorio del Roque de los Muchachos. The detector was a GEC P8603 CCD with 385×578 pixels, oriented with its long axis in the dispersion direction. A 150 g mm^{-1} grating was used in first order, yielding a dispersion of $2.9 \text{ \AA pixel}^{-1}$, with wavelength coverage from 5290 to 6840 \AA . The resolution of these spectra was 7 \AA , as judged from the FWHM of comparison arc lines. The slit width was $105 \text{ }\mu\text{m}$, which projected to 0.54 arcsec on the sky, while the pixel size perpendicular to the dispersion was 0.30 arcsec. Spectra were obtained of P Cygni itself (0.5-s exposure time) and at offset positions 3, 6 and 9 arcsec east of P Cygni (with exposure times of 5, 100 and 1000 s, respectively), all with a slit position angle of 0° (north-south). The seeing, as determined from the FWHM of the stellar continuum at 6590 \AA in the on-star spectral image, was 1.6 arcsec.

In addition, blue spectra of the 3623–3823 \AA wavelength region, encompassing the $[\text{O II}]\lambda\lambda 3726, 3729 \text{ \AA}$ doublet, were obtained on 1988 October 12 UT. A 1200 g mm^{-1} grating was used in first order, yielding a dispersion of $0.37 \text{ \AA pixel}^{-1}$ and a resolution of 0.75 \AA . The slit width was $150 \text{ }\mu\text{m}$, projecting to 0.81 arcsec on the sky, while the pixel size perpendicular to the dispersion was 0.30 arcsec, as before. The slit was oriented north-south and spectra were obtained of P Cygni (30-s exposure time) and at offset positions 6 and 9 arcsec to the east of P Cygni (with exposure times of 300 and 900 s, respectively).

The CCD images were debiased and flat-fielded in the standard way using the STARLINK data reduction package FIGARO. Each two-dimensional spectrum was then wavelength calibrated using Cu-Ar arcs which were interspersed between the target observations. All spectra were flux calibrated, using standard-star observations of LDS 749B (Oke 1974) for the red spectra and BD + 28 $^\circ$ 4211 (Massey *et al.* 1988) for the blue spectra. Subsequent data analysis was performed using the STARLINK package DIPSO.

3 SPECTRAL AND SPATIAL ANALYSIS

3.1 Spectral analysis

The spatial dimension of the long-slit spectra was first collapsed to provide maximum signal-to-noise ratio. The spectrum obtained at each offset position was then compared to the spectrum of P Cygni itself in the region of the nebular lines $[\text{N II}]\lambda\lambda 6548, 6548 \text{ \AA}$ and $[\text{S II}]\lambda\lambda 6716, 6731 \text{ \AA}$. The results are shown in Figs 1 and 2 and are influenced by two observational factors: the spectra at smaller offsets are increasingly dominated by the seeing disc of P Cygni itself, while the spectra at larger offsets were able to go progressively deeper without saturating the detector. Figs 1(a), (b) and (c) show the region around $\text{H}\alpha$ and the $[\text{N II}]\lambda\lambda 6548, 6584 \text{ \AA}$ lines at the 3-, 6- and 9-arcsec offset positions, respectively. One can see a progression in the contrast of the $[\text{N II}]\lambda\lambda 6584 \text{ \AA}$ line with increasing offset. There is no discernible excess at the 3-arcsec offset position, a marginal excess at the 6-arcsec offset position and a strong excess at the 9-arcsec offset. As expected, the $[\text{N II}]\lambda\lambda 6584 \text{ \AA}$ line is much weaker and only shows an excess at the 9-arcsec offset position. We detected $[\text{N II}]\lambda\lambda 5755 \text{ \AA}$ emission in our on-star spectrum of P Cygni [see also fig. 4 of Stahl *et al.* (1991)], but its equivalent width at the 9-arcsec offset position (0.5 \AA)

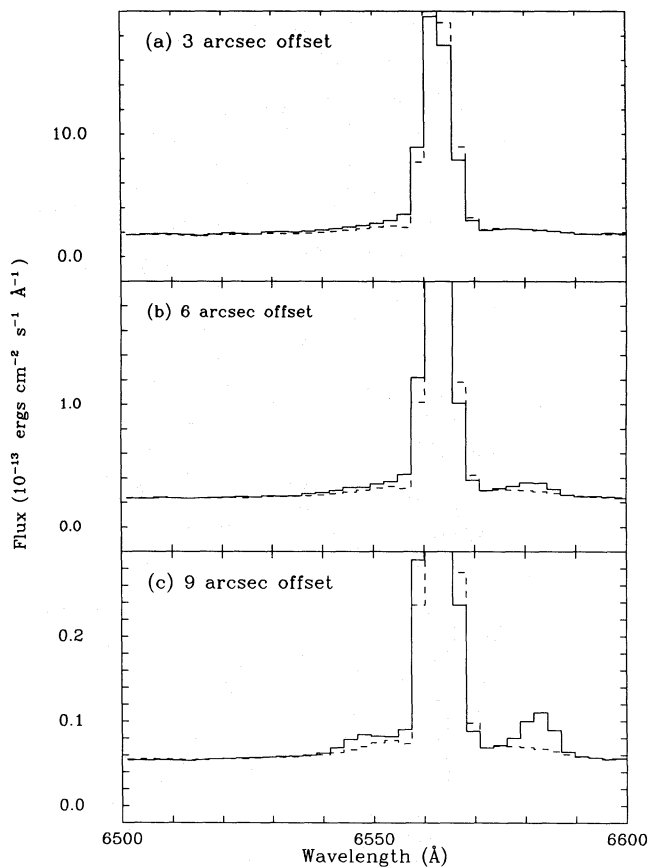


Figure 1. (a), (b) and (c) show the comparison between the stellar and off-star spectra in the $\text{H}\alpha$, $[\text{N II}]$ region, for the 3-, 6- and 9-arcsec offset positions, respectively. The dashed line in all plots is P Cygni's on-star spectrum, scaled down to match the continuum of the offset spectrum, while the solid line is the offset spectrum itself.

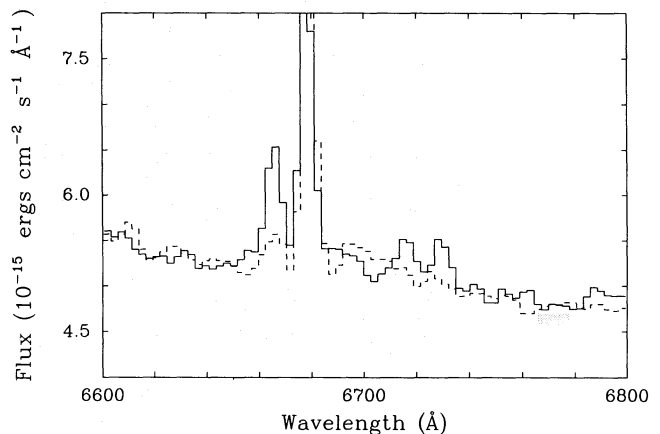


Figure 2. A comparison of the 9-arcsec offset spectrum (solid line) and the on-star spectrum (dashed line) in the region of $[\text{Ni II}]\lambda\lambda 6667, 6667 \text{ \AA}$ and $[\text{S II}]\lambda\lambda 6716, 6731 \text{ \AA}$.

was the same as in the on-star spectrum, allowing us to place only an upper limit to any $[\text{N II}]\lambda\lambda 5755 \text{ \AA}$ nebular emission at the offset position.

The $[\text{S II}]\lambda\lambda 6716, 6731 \text{ \AA}$ lines were weaker than the $[\text{N II}]\lambda\lambda 6584 \text{ \AA}$ line and are only detected at the 9-arcsec offset posi-

tion (Fig. 2), the observed wavelengths agreeing with those of the [S II] doublet.

Also apparent in Fig. 2 is a relatively strong emission feature at 6666 Å, which we identify with [Ni II] 6666.8 Å. It appears to be weakly present in the on-star spectrum (dashed line in Fig. 2) but is much stronger at the 9-arcsec offset position (solid line in Fig. 2), whereas the nearby He I 6678.1 Å emission line has the same equivalent width in both spectra, indicating that there is no nebular component to the He I line at the 9-arcsec offset position. An analysis of the spatial profile of the [Ni II] emission along the slit at the 9-arcsec offset position shows that it is similar to that exhibited by [N II] 6584 Å (see next section), confirming that it arises from extended nebular emission.

The nebular component of the [Ni II] 6666.8 Å line is as strong as the combined [S II] doublet. The relative strengths of the [Ni II] and [S II] lines at the 9-arcsec offset position are similar to those found in the 1984 August maximum-phase spectrum of the LBV S Dor (Stahl & Wolf 1986; their fig. 4). The [N II] 6584 and 5755 Å lines were also strong in the spectrum of S Dor at that time. [Ni II] 6666.8 Å was also very strong in the 1984 August spectrum taken by Stahl & Wolf (1986) of the S Dor variable R 71 (=HDE 269006), its intensity rivalling that of [N II] 6584 Å. We shall return to the question of the excitation of the [Ni II] line in Section 4.

3.2 Spatial analysis

No signal attributable to nebular emission was detected at the 3-arcsec offset position and only a marginal excess was found for the [N II] 6584 Å line in the 6-arcsec offset spectrum. When the signal shown in Fig. 1(b) is spread out over the spatial profile it is too weak to yield useful information. Such was not the case for the distribution along the slit at the 9-arcsec offset position (Fig. 1c).

For the 9-arcsec offset spectrum, we have derived the surface-brightness distributions along the slit for wavelength bands centred on H α and [N II] 6584 Å and for symmetrically spaced continuum bands on either side of these lines. The wavelength ranges of these bands are listed in Table 1. Imperfect charge transfer when the CCD was read out meant that some of the H α signal ‘leaked’ to the blue, affecting the region containing [N II] 6548 Å. To allow for this, the broad wavelength region used for the on-line H α band included the two [N II] lines as well. The distribution derived for this band was ultimately corrected for the [N II] contribution by subtracting the derived [N II] 6584 Å distribution (multiplied by 1.340 to allow for both the 6584 and 6548 Å lines).

The extracted brightness distributions along the slit are due to a combination of the effects of P Cygni’s seeing disc plus intrinsic nebular emission. We corrected for the seeing-disc component in the following manner. Using the spectrum of P Cygni itself, we measured the flux in each on-line and continuum band and derived the emission per unit Å in each band. Emission detected at any offset position due purely to the stellar seeing disc should have the same line-to-continuum ratio as the on-star spectrum. For the 9-arcsec offset spectrum, we therefore averaged the surface-brightness distributions per unit Å along the slit for the continuum bands on either side of each line, scaled the resulting profile up by a factor equal to the on-star line-to-continuum ratio and subtracted it from the on-line profile. This procedure

should take out any line and continuum contribution resulting from the stellar seeing disc, leaving only the nebular line emission contribution. Finally, the derived on-line brightness profiles (per pixel per Å) were multiplied by the width of the on-line band in Å (Table 1) and divided by the pixel size of 0.1642 arcsec² to produce the emission-line surface-brightness distributions, in erg cm⁻² s⁻¹ arcsec⁻², that are shown in Fig. 3(a) and (b) for [N II] 6584 Å and H α . Fig. 3(c) over-plots the H α and [N II] distributions, showing that the lines have similar strengths.

Table 1. Wavelength ranges for the bands used to derive surface-brightness distributions.

Line	On-line Band (Å)	Continuum Band 1 (Å)	Continuum Band 2 (Å)
[N II] 6584	6573–6591	6510–6532	6634–6655
H α	6502–6618	6465–6500	6621–6656

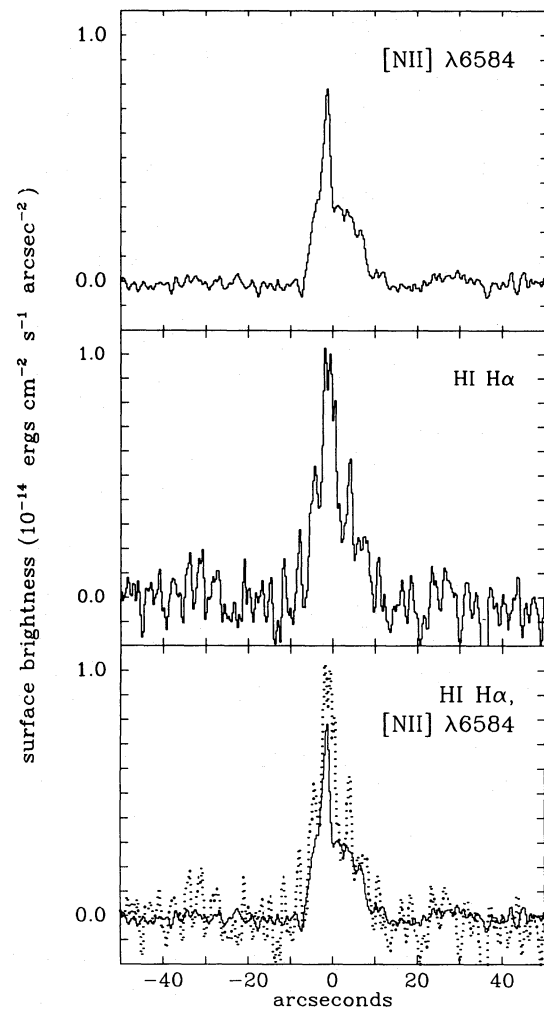


Figure 3. Spatial surface-brightness profiles along the slit at the 9-arcsec offset position. Upper: [N II] λ 6584; middle: H α ; lower: a superposition of H α (solid line) and [N II] λ 6584 (dotted line). The plots run from north (negative) to south (positive).

The nebular line brightness profiles along the 9-arcsec slit that are presented in Fig. 3 demonstrate immediately that the emission does not arise from a uniform surface-brightness region. The peak $H\alpha$ and $[N\ II]$ surface brightnesses in Fig. 3, corresponding to the minimum angular separation from P Cygni of 9 arcsec, are about a factor of 3 lower than the levels predicted by an extrapolation to 9 arcsec of Leitherer & Zickgraf's (1987) azimuthally averaged surface-brightness profiles. The peak surface brightness of $H\alpha$ at the 9-arcsec offset position is about 15 times lower than the mean $H\alpha$ surface brightness of the AG Car nebula implied by Stahl's (1987) data. This, coupled with the fact that P Cyg is 2–3 mag brighter than AG Car, explains why the P Cyg nebulo- sity has hitherto escaped detection.

3.3 Relative line intensities

Table 2 presents the observed and dereddened nebular line strengths measured for the central 28-arcsec portion of the 9-arcsec offset long-slit spectrum. The $[N\ II]$ 6584 Å and $[S\ II]$ fluxes were measured from the net spectrum described in Section 3.1. In each case the spectrum of P Cygni was scaled to match the continuum levels in the adjacent wave-length regions of each offset spectrum and then subtracted. The upper limit to the strength of any nebular $[N\ II]$ 5755 Å emission was also obtained from this spectrum. The upper limit to the strength of $[O\ II]$ 3726, 3729 Å was obtained in a similar manner from the 9-arcsec offset blue spectrum. The strength of nebular $H\alpha$ relative to the other lines was not estimated from the net flux spectrum described in Section 3.1, because the contribution from the strong stellar $H\alpha$ seeing component was found to be very sensitive to the exact continuum normalization of the stellar spectrum to the offset spectrum (the other lines were far less sensitive to this). Instead, we determined the relative strengths of nebular $H\alpha$ and $[N\ II]$ 6584 Å by integrating and ratioing the surface-brightness distributions shown in Fig. 3 (the manner of their derivation using broad continuum bands reduces the continuum normalization uncertainty). The strengths of the $[S\ II]$ lines relative to $[N\ II]$ 6584 Å are estimated to be accurate to about 15 per cent, whereas the strength of $H\alpha$ relative to the other lines is estimated to be accurate to only about 35 per cent.

The observed line fluxes listed in Table 2 correspond to the mean surface brightness in each line over the central 91 spatial increments (27.7 arcsec) of the 9-arcsec offset spectra. In order to put them on the usual scale where $H\beta = 100$, the dereddened line intensities listed in Table 2 have been normalized so that $H\alpha$ has its Case B recombination value of 285 corresponding to $T_e = 10^4$ K and $n_e = 10^3$ cm⁻³ (Hummer & Storey 1987). The adopted value for the reddening to P Cygni was $E(B - V) = 0.60$ (Deacon & Barlow 1991).

4 NEBULAR ABUNDANCE ANALYSIS

Using the Gaussian-fitting routine `ELF` within `DIPSO`, we have measured the flux ratio for $[S\ II]$ 6716/6731 to be 0.96 ± 0.05 . For an electron temperature lying between 4000 and 10 000 K (see below), this $[S\ II]$ ratio implies an electron density of 600 ± 150 cm⁻³ (we used the atomic data tabulated by Mendoza (1983) for this and subsequent statistical

Table 2. Observed and dereddened nebular line intensities.

Ion	Wavelength (Å)	Observed (ergs cm ⁻² s ⁻¹ arcsec ⁻²)	Dereddened ($H\beta = 100$)
$[O\ II]$	3727	$<4.7 \times 10^{-16}$	<204
$[N\ II]$	5755	$<6.7 \times 10^{-17}$	<11.8
$H\alpha$	6563	2.08×10^{-15}	285
$[N\ II]$	6584	2.08×10^{-15}	283
$[N\ i\ II]$	6667	6.4×10^{-15}	86
$[S\ II]$	6716	2.62×10^{-16}	34.4
$[S\ II]$	6731	2.60×10^{-16}	34.1

Table 3. Nitrogen, oxygen and sulphur abundances.

T (K)	N^+/H^+	O^+/H^+	S^+/H^+	N^+/S^+
4000	2.10×10^{-3}	$<4.2 \times 10^{-2}$	6.11×10^{-5}	34.3
4500	1.09×10^{-3}	$<1.4 \times 10^{-2}$	3.22×10^{-5}	33.9
5000	6.44×10^{-4}	$<5.5 \times 10^{-3}$	1.92×10^{-5}	33.5
5500	4.17×10^{-4}	$<2.6 \times 10^{-3}$	1.25×10^{-5}	33.2
6000	2.89×10^{-4}	$<1.6 \times 10^{-3}$	8.76×10^{-6}	32.9
6500	2.11×10^{-4}	$<8.3 \times 10^{-4}$	6.46×10^{-6}	32.7
7000	1.61×10^{-4}	$<5.3 \times 10^{-4}$	4.97×10^{-6}	32.4
7500	1.27×10^{-4}	$<3.5 \times 10^{-4}$	3.95×10^{-6}	32.2
8000	1.03×10^{-4}	$<2.5 \times 10^{-4}$	3.23×10^{-6}	31.9
8500	8.56×10^{-5}	$<1.8 \times 10^{-4}$	2.70×10^{-6}	31.7
9000	7.24×10^{-5}	$<1.4 \times 10^{-4}$	2.30×10^{-6}	31.4
9500	6.22×10^{-5}	$<1.1 \times 10^{-4}$	1.99×10^{-6}	31.2
10000	5.42×10^{-5}	$<8.5 \times 10^{-5}$	1.75×10^{-6}	30.9

equilibrium calculations). Our upper limit for the ratio $[N\ II]$ 5755/6584 provides an upper limit to the electron temperature of 16 000 K. Table 3 lists, for a range of electron temperatures between 4000 and 10 000 K, the derived ionic abundance ratios for N^+/H^+ , O^+/H^+ and S^+/H^+ . Provided the nebula is only photoionized, it is unlikely that higher ionization stages of N, O or S exist around P Cygni, whose effective temperature is 18 000–20 000 K (Barlow & Cohen 1977; Lamers, de Groot & Cassatella 1983; Deacon & Barlow 1991). Drew (1985) modelled the detailed ionization structure of the wind of P Cygni and found that these elements were only singly ionized throughout the wind.

Although the derived N, O and S abundances relative to hydrogen are strongly temperature dependent (Table 3), the N/S ratio is not, due to the very similar excitation energies of the $[N\ II]$ 6584 Å and $[S\ II]$ 6716, 6731 Å transitions. The last column of Table 3 shows that the derived N^+/S^+ ratio varies between only 34 and 31 when the adopted electron temperature is varied between 4000 and 10 000 K.

The initial abundance of sulphur in the outer layers of massive stars is not expected to be altered by any evolu-

tionary nuclear process, so the abundance of sulphur around P Cygni should be similar to that found in the Sun and in galactic H II regions. The solar S/H ratio is 1.6×10^{-5} (Grevesse & Anders 1989), while that for the Orion nebula is 1.3×10^{-5} (Baldwin *et al.* 1991). From inspection of the fourth column of Table 3, a similar sulphur abundance at the P Cygni 9-arcsec offset position would imply an electron temperature of about 5300 K. The N/H abundance (column 2 of Table 3) would then be about 5×10^{-4} , while the oxygen abundance is not significantly constrained, the upper limit (column 3) being well above solar.

We used the Ni⁺ atomic data of Nussbaumer & Storey (1982) to estimate the Ni⁺ abundance. The [Ni II] 6666.8 Å line also has a similar excitation energy to the [S II] 6716, 6731 Å lines and so Ni⁺/S⁺ abundances derived assuming collisional excitation for both species are not sensitive to the adopted electron temperature. However, we then derive a Ni⁺/S⁺ ratio of 270, compared to only 0.11 for the Sun (Grevesse & Anders 1989). If the nebular parameters discussed above were valid ($n_e = 600 \text{ cm}^{-3}$, $T_e \approx 5300 \text{ K}$), the derived Ni/H ratio would be 4×10^{-3} . Clearly such nickel abundances are impossible to countenance and we conclude that the observed [Ni II] 6666.8 Å line is not the result of collisional excitation in a low-density, low-temperature medium. A quantitative analysis of the [Ni II] and [S II] emission lines seen in the spectrum of S Dor (Stahl & Wolf 1986) would probably lead to the same conclusion. It is worth noting that anomalously strong [Ni II] 7377 Å emission (which originates from the same term as $\lambda 6666.8$) has been seen in the spectra of supernova remnants, Herbig–Haro objects and the Orion nebula (Dennefeld 1986; Henry & Fesen 1988), yielding Ni/Fe ratios up to 10 times solar when compared to [Fe II] lines of similar excitation energy. The critical density of the [Ni II] $\lambda 6666.8$ transition is $\sim 10^7 \text{ cm}^{-3}$, so in principle its strength could be enhanced by emission from high-density knots. However, the [N II] $\lambda 5755$ transition would also be strongly enhanced by such a process, whereas we have failed to detect any emission from this transition at the offset positions in excess of the scattered stellar contribution, in contrast to the situation for [Ni II] $\lambda 6666.8$. Fluorescent excitation of the [Ni II] line seems the most attractive explanation for its strength but Henry & Fesen (1988) were unable to identify any Ni II resonance transition to a higher state that was coincident with a well-known line of another species that could act as the pump. For the nebular parameters derived here, the [Ni II] 7378/6667 flux ratio is predicted to be between 15 and 20 if both lines are collisionally excited. If, on the other hand, fluorescence is responsible, the 7378/6667 ratio would be expected to be closer to the statistical equilibrium value of 2.8.

5 DISCUSSION

Table 4 presents a comparison of the N/S abundance ratios, by number, found for the Sun, the Orion nebula and P Cygni. Also listed are the N/S ratios found for two other galactic LBVs, AG Car and HR Car. The N/S ratio listed for AG Car is that derived by Mitra & Dufour, (1990), while that listed for HR Car has been derived by us from the dereddened [N II] 6548, 6584 Å and [S II] 6716, 6731 Å line fluxes measured for the HR Car nebula by Hutsemekers & Van Drom (1991). The N/S ratios for the three LBVs are 5–10 times larger than found for solar or Orion-nebula material.

Table 4. Abundance ratio comparisons.

Environment	Ref.	N/S	(C+N)/S	(C+N+O)/S
Solar	a	6.2	31	83
Orion	b	7.3	35	73
P Cyg	c	33	-	-
AG Car	d	63	-	-
HR Car	e,c	63	-	-

References: (a) Grevesse & Anders (1989), Grevesse *et al.* (1990, 1991); (b) average of Baldwin *et al.* (1991) and Rubin *et al.* (1991); (c) this paper; (d) Mitra & Dufour (1990); (e) Hutsemekers & Van Drom (1991).

Massive stars generate their initial luminosity from the CNO bi-cycle. The CN cycle achieves equilibrium first, converting most of the original carbon into nitrogen. The CNO cycle takes longer to achieve equilibrium and can ultimately convert most of the original oxygen into nitrogen. The degree to which these processes will have advanced in currently exposed surface layers will depend on how quickly the outer layers have been removed. Columns 4 and 5 of Table 4 list the (C+N)/S and (C+N+O)/S abundance ratios measured for the Sun and the Orion nebula. The N/S ratio of 33 found for the P Cygni circumstellar nebula closely matches the (C+N)/S ratios found for the Sun and the Orion nebula, indicating that it is composed of material in which most of the original carbon has been converted into nitrogen by the CN cycle. The AG Car and HR Car nebulae both have an N/S ratio of 63, too high to be due to the C N cycle alone but consistent with material in which the CNO bi-cycle has additionally converted a large fraction of the original oxygen into nitrogen.

However, this straightforward interpretation is not possible in the case of the AG Car nebula, since the sulphur and oxygen abundances derived by Mitra & Dufour (1990) were 30 times below solar for the case of their preferred nebular electron temperature of 9000 K. Even if one treats the electron temperature of the AG Car nebula as a free parameter (on the grounds that all of Mitra and Dufour's [N II] $\lambda 5755$ measurements were uncertain), problems still remain. An electron temperature sufficiently low to yield a cosmic S⁺ abundance for the AG Car nebula (4000–4500 K), would simultaneously imply an oxygen abundance that was 2–5 times cosmic. An electron temperature of just under 5000 K for the AG Car nebula would yield a cosmic abundance for oxygen and an N/O ratio consistent with CN cycling alone, along with an S⁺ abundance that was about half cosmic. It is possible that some sulphur in the AG Car nebula is in the form of S²⁺, produced either by photoionization when the star was in a high-excitation state, or by shocks. A search for the $\lambda\lambda 9069, 9532$ lines of [S III] from the AG Car nebula could help resolve this question. The detection of these lines in the spectrum of the nebula around P Cyg would indicate a shock-excitation origin since, as discussed in the previous section, its current spectral type (which is not thought to have varied significantly in the past 100 yr) is of too low excitation to produce significant S²⁺ by photoionization.

We showed in Section 4 that a nebular electron temperature of ~ 5300 K would yield a Solar–Orion S/H abundance for the P Cyg nebula, and it would also yield an N/H ratio consistent with CN cycling of carbon into nitrogen. Although N II is the dominant heavy-element species in the stellar spectrum of P Cygni, carbon is not completely absent in the surface layers, since the $\lambda\lambda 6577.8, 6582.7$ lines of C II were found to be in emission in the H α -region spectrum of P Cygni presented by Bernat & Lambert (1978). The 1984 August spectrum of the H α region of AG Car (Viotti *et al.* 1991) also shows these two C II lines in emission, despite its circumstellar nebula also indicating an advanced stage of nuclear processing. By 1987 June however, when AG Car's spectrum had changed to Of/WN9 from the B[e] type of 1984 August, Viotti *et al.* found that the narrow C II emission lines had given way to broad [N II] 6584 Å emission. Therefore at least small amounts of carbon are left in the surface layers of both P Cyg and AG Car.

From an analysis of its infrared recombination-line spectrum, Barlow (1991) has derived a He/H ratio of 0.5 by number for P Cygni. The evolutionary tables of Maeder (1990) indicate that for a star with initial solar abundances and an initial mass of 40–85 M_{\odot} the surface carbon abundance should have dropped by a factor of about 30 when the surface hydrogen mass fraction has fallen to 0.33–0.50. However, the same models predict that the surface oxygen abundance should have fallen by a factor of at least 3 by that stage, whereas the N/S ratio we have derived for the P Cyg nebula, when compared to the solar or Orion (C+N)/S values (Table 4), indicates that this has not happened. A direct measurement of the oxygen abundance in the P Cyg nebula would therefore be of some interest.

For a distance to P Cyg of 1.8 kpc, the centre of the 9-arc-sec offset slit would have corresponded to a separation of 2.4×10^{17} cm from the star. From radio flux measurements of \dot{M}/v_{∞} , the steady mass-loss rate from P Cygni (see Barlow 1991) would give an electron density of only 18 cm^{-3} at this distance, compared to the value of 600 cm^{-3} determined from the [S II] doublet ratio. One possibility could be that the detected emission comes from material ejected during P Cyg's outburst in 1600. If this was the case, the required expansion velocity would be 200 km s^{-1} , virtually the same as the current wind terminal velocity of 206 km s^{-1} (Lamers, Korevaar & Cassatella 1985). On the other hand, the nebulosities found around other LBVs have significantly lower expansion velocities than this, e.g. 70 km s^{-1} for the AG Car nebula (Smith 1991) and $30\text{--}50 \text{ km s}^{-1}$ for the circumstellar nebulae around LBVs in the LMC (Walborn 1982; Stahl & Wolf 1986). With the detection of the P Cygni nebula, all four confirmed galactic LBVs (P Cyg, η Car, AG Car and HR Car) have been shown to possess nebulae. Clearly, a determination of the expansion velocity and full morphology of the nebulosity around P Cygni could help establish the relation between this classical object and other luminous blue variables.

ACKNOWLEDGMENTS

DRHJ acknowledges the award of an SERC Studentship and JED the award of an SERC Advanced Fellowship. We thank Dr L. J. Smith and Dr C. Leitherer for their comments on an earlier draft of this paper.

REFERENCES

- Baars, J. W. M. & Wendker, H. J., 1987. *Astr. Astrophys.*, **181**, 210.
 Baldwin, J. A., Ferland, G. J., Martin, P. G., Corbin, M. R., Cota, S. A., Peterson, B. M. & Sletteback, A., 1991. *Astrophys. J.*, **374**, 580.
 Barlow, M. J., 1991. *Wolf-Rayet Stars and Interrelations with other Massive Stars in Galaxies*, IAU Symp. No. 143, p. 281, eds van der Hucht, K. A. & Hidayat, B., Kluwer, Dordrecht.
 Barlow, M. J. & Cohen, M., 1977. *Astrophys. J.*, **213**, 737.
 Bernat, A. P. & Lambert, D. L., 1978. *Publ. astr. Soc. Pacif.*, **90**, 520.
 Davidson, K., Moffat, A. F. J. & Lamers, H. J. G. L. M., eds, 1989. *Physics of Luminous Blue Variables*, Kluwer, Dordrecht.
 Davidson, K., Dufour, R. J., Walborn, N. R. & Gull, T. R., 1986. *Astrophys. J.*, **305**, 867.
 Deacon, J. R. & Barlow, M. J., 1991. *Wolf-Rayet Stars and Interrelations with other Massive Stars in Galaxies*, IAU Symp. No. 143, p. 558, eds van der Hucht, K. A. & Hidayat, B., Kluwer, Dordrecht.
 Dennefeld, M., 1986. *Astr. Astrophys.*, **157**, 267.
 Drew, J. E., 1985. *Mon. Not. R. astr. Soc.*, **217**, 867.
 Grevesse, N. & Anders, E., 1989. In: *Cosmic Abundances of Matter*, AIP Conf. Proc. 183, p. 1, ed. Waddington, C. J., American Institute of Physics, New York.
 Grevesse, N., Lambert, D. L., Sauval, A. J., van Dishoeck, E. F., Farmer, C. B. & Norton, R. H., 1990. *Astr. Astrophys.*, **232**, 225.
 Grevesse, N., Lambert, D. L., Sauval, A. J., van Dishoeck, E. F., Farmer, C. B. & Norton, R. H., 1991. *Astr. Astrophys.*, **242**, 488.
 Henry, R. B. C. & Fesen, R. A., 1988. *Astrophys. J.*, **329**, 693.
 Hummer, D. G. & Storey, P. J., 1987. *Mon. Not. R. astr. Soc.*, **224**, 801.
 Humphreys, R. M., 1989. In: *Physics of Luminous Blue Variables*, p. 3, eds Davidson, K., Moffat, A. F. J. & Lamers, H. J. G. L. M., Kluwer, Dordrecht.
 Hutsemekers, D. & Van Drom, E., 1991. *Astr. Astrophys.*, **248**, 141.
 Lamers, H. J. G. L. M., de Groot, M. & Cassatella, A., 1983. *Astr. Astrophys.*, **128**, 299.
 Lamers, H. J. G. L. M., Korevaar, P. & Cassatella, A., 1985. *Astr. Astrophys.*, **149**, 29.
 Leitherer, C. & Zickgraf, F. J., 1987. *Astr. Astrophys.*, **174**, 103.
 Maeder, A., 1990. *Astr. Astrophys. Suppl.*, **84**, 139.
 Massey, P., Strobel, K., Barnes, J. W. V. & Anderson, E., 1988. *Astrophys. J.*, **328**, 315.
 Mendoza, C., 1983. *Planetary Nebulae*, IAU Symp. No. 103, p. 143, ed. Flower, D. R., Reidel, Dordrecht.
 Mitra, P. M. & Dufour, R. J., 1990. *Mon. Not. R. astr. Soc.*, **242**, 98.
 Nussbaumer, H. & Storey, P. J., 1982. *Astr. Astrophys.*, **110**, 295.
 Oke, J. B., 1974. *Astrophys. J. Suppl.*, **27**, 21.
 Rubin, R. H., Simpson, J. P., Haas, M. R. & Erickson, E. F., 1991. *Astrophys. J.*, **374**, 564.
 Smith, L. J., 1991. *Wolf-Rayet Stars and Interrelations with other Massive Stars in Galaxies*, IAU Symp. No. 143, p. 385, eds van der Hucht, K. A. & Hidayat, B., Kluwer, Dordrecht.
 Stahl, O., 1987. *Astr. Astrophys.*, **182**, 229.
 Stahl, O., 1989. In: *Physics of Luminous Blue Variables*, p. 149, eds Davidson, K., Moffat, A. F. J. & Lamers, H. J. G. L. M., Kluwer, Dordrecht.
 Stahl, O. & Wolf, B., 1986. *Astr. Astrophys.*, **158**, 371.
 Stahl, O., Mandel, H., Szeifert, Th., Wolf, B. & Zhao, F., 1991. *Astr. Astrophys.*, **244**, 467.
 Viotti, R., Baratta, G. B., Rossi, C. & di Fazio, A., 1991. *Wolf-Rayet Stars and Interrelations with other Massive Stars in Galaxies*, IAU Symp. No. 143, p. 499, eds van der Hucht, K. A. & Hidayat, B., Kluwer, Dordrecht.
 Walborn, N. R., 1982. *Astrophys. J.*, **256**, 452.
 Wendker, H. J., 1982. *Astr. Astrophys.*, **116**, L1.